ACS Combinatorial Science

Research Article

pubs.acs.org/acscombsci

# Combinatorial High-Throughput Optical Screening of High Performance Pd Alloy Cathode for Hybrid Li−Air Battery

Young Jin Jun,[†,§] Sung Hyeon Park,[†,§] and Seong Ihl Woo*[,†,‡]

[†]Department of Chemical and Biomolecular Engineering, Korea Advanced Institute of Science and Technology, Daejeon, 305-701, Republic of Korea

[‡]Graduate School of EEWS (BK21PLUS), Korea Advanced Institute of Science and Technology, Daejeon, 305-701, Republic of Korea

Supporting Information

**ABSTRACT:** Combinatorial high-throughput optical screening method was developed to find the optimum composition of highly active Pd-based catalysts at the cathode of the hybrid Li−air battery. Pd alone, which is one-third the cost of Pt, has difficulty in replacing Pt; therefore, the integration of other metals was investigated to improve its performance toward oxygen reduction reaction (ORR). Among the binary Pd-based catalysts, the composition of Pd−Ir derived catalysts had higher performance toward ORR compared to other Pd-based binary combinations. The composition at 88:12 at. % (Pd: Ir) showed the highest activity toward ORR at the cathode of the hybrid Li−air battery. The prepared $Pd_{88}Ir_{12}$/C catalyst showed a current density of −2.58 mA $cm^{-2}$ at 0.8 V (vs RHE), which was around 30% higher compared to that of Pd/C (−1.97 mA $cm^{-2}$). When the prepared $Pd_{88}Ir_{12}$/C catalyst was applied to the hybrid Li−air battery, the polarization of the cell was reduced and the energy efficiency of the cell was about 30% higher than that of the cell with Pd/C.

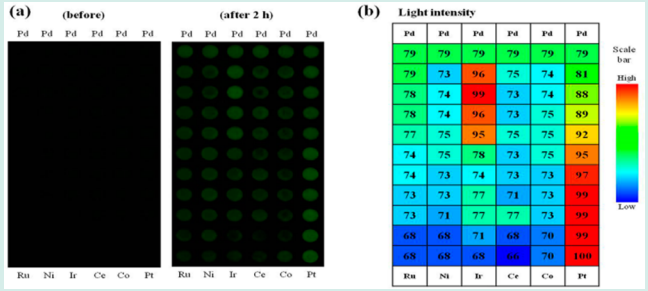


**KEYWORDS:** *combinatorial high-throughput method, optical screening, cathode of Li−air battery, hybrid Li−air battery*

## INTRODUCTION

Theoretically, the Li−air battery has a higher energy density than that of a Li-ion battery,[1] since the capacity is provided by the inexhaustible $O_2$ from air that is supplied to the cathode, continuously. Therefore, the Li−air battery has been investigated as a highly potential candidate among the rechargeable batteries for the use in electric vehicles.[2] Within the two main Li−air battery systems, there are issues such as the deposition of insoluble discharge product ($Li_2O_2$) on the porous cathode,[3] the decomposition of an organic electrolyte,[4] and the protection of the Li metal anode from moisture.[5] To overcome these drawbacks, the hybrid system composed of the organic electrolyte in the anode side (oxidation of Li to $Li^+$) and the aqueous electrolyte in the cathode side (reduction of oxygen in the presence of $Li^+$) was manufactured.[6,7] Because of the slow kinetics of oxygen reduction reaction (ORR), the electrocatalyst at the cathode reaction plays a vital role in determining the battery performance such as power density, cycling capability, and energy efficiency.[8−10] A diverse selection of materials have been used as a cathode catalyst and these materials can be classified into the following four groups: noble metal based catalysts,[9,11−13] carbonaceous material,[14,15] transition metal oxides,[16−18] and inorganic−organic composites.[19−21]

It has been reported that Pt and Pt-based catalysts have been intensively studied as an electrocatalyst due to their high stability and superior electrocatalytic performance.[12,22−31] However, the scarcity and the cost of Pt encourage the search for alternative catalysts. Among the noble metals, Pd shows a relatively good performance toward ORR.[22] Pd alone has a lower ORR performance than that of Pt in the field of fuel cells; therefore, Pd-based catalysts have been investigated through the interaction with other transition metals to improve the ORR performance.[23−27]

Pd-based catalysts can be prepared through various combinations and compositions; thus, time and labor force is of great need. A methodology called the combinatorial high-throughput screening was applied to overcome this issue. Combinatorial high-throughput screening has been introduced in the field of fuel cells in the late 1990s as a highly potential methodology to find optimized compositions among various combinations of catalysts.[28−31] Since then, many groups reported the use of this method to find optimum compositions of catalyst having outstanding performance toward ORR.[29,30,32−40] In our group, this methodology was used to investigate various optimized catalysts in the field of fuel cells.[22,29−31,41] However, this experiment was targeted to hybrid Li−air battery, therefore, the entire combinatorial system was

**Received:** March 10, 2014
**Revised:** July 11, 2014
**Published:** November 5, 2014

   dx.doi.org/10.1021/co500041n | ACS Comb. Sci. 2014, 16, 670−677

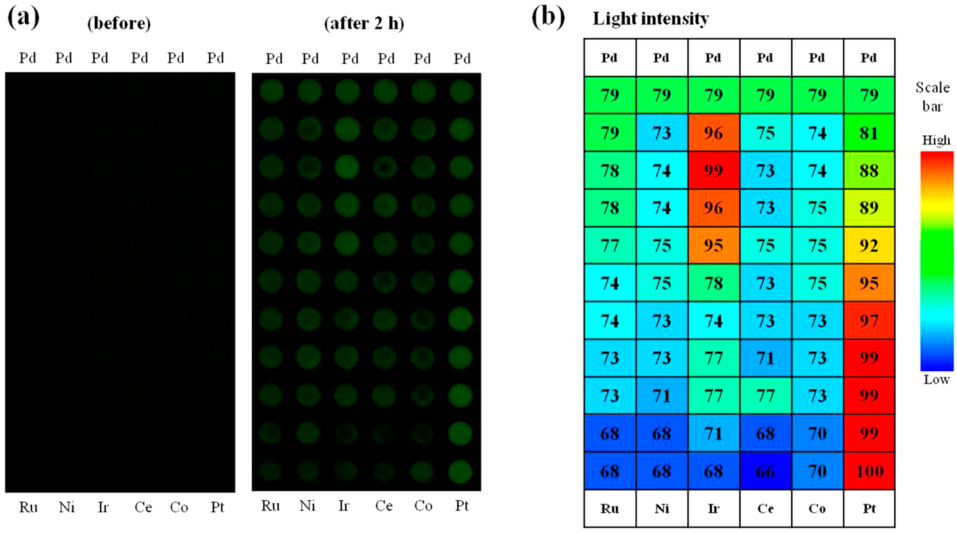


**Figure 1.** (a) Images from optical screening for Pd based array at a constant potential of 0.8 V (vs RHE); before (left) and after 2 h (right). (b) Degree of brightness of catalyst spots.

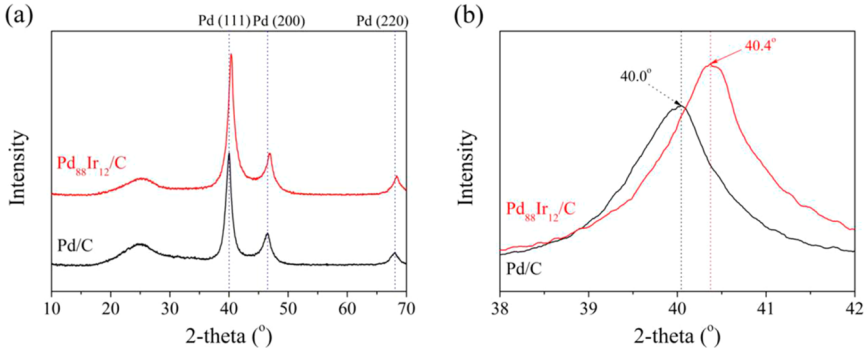


**Figure 2.** (a) XRD patterns of the prepared catalysts: Pd/C and $Pd_{88}Ir_{12}/C$. (b) Magnified intense Pd peaks of the prepared catalysts between 38 to 42°.

performed in the presence of $Li^+$, similar to that of the cathode in the hybrid Li−air battery (overall reaction $4Li + O_2 + 4H^+ \rightarrow 4Li^+ + 2H_2O$, acidic media), distinct from fuel cell (overall reaction $2H_2 + O_2 \rightarrow 2H_2O$). Moreover, many combinations and compositions of Pd with other transition metals were investigated at different $Li^+$ concentrations, we chose the optimum composition of Pd-based catalysts through combinatorial high-throughput screening, and the selected composition was prepared into single catalyst for a thorough characterization of its performance in the hybrid Li−air battery.

## RESULTS AND DISCUSSION

To investigate the performance trend of ORR activity within the Pd-based catalysts in combinatorial array, the optical screening method was performed. The images from optical screening analysis for the combinatorial array of Pd-based catalysts are shown in Figure 1a and Supporting Information Figure S1. A constant potential of 0.8 V (vs RHE) was applied to the combinatorial array in optical screening for 2 h, and the brightness of each spot was assessed. Spots emitting higher brightness represent that the catalysts have relatively higher ORR performance compared to the other catalyst spots. The brightness between spots was difficult to be differentiated with the naked eye in the fluorescence images. For a clearer comparison in brightness between the catalyst spots, the brightness of each spot was measured using photoshop and represented in a 2D-graph as shown in Figure 1b.

The red color defines higher catalytic activity toward ORR compared to the blue color regions, as described in the scale of the figure. Catalyst spots at the combinations of Pd−Pt emitted higher brightness compared to other spots. From previous report by Lim et al.,[13] the ORR performance of Pd−Pt based catalysts demonstrated outstanding activity toward ORR compared to other Pd-transition metal combinations, and this is consistent with the results of the optical screening analysis of the combinatorial array. Not only the combinations of Pd−Pt, but the catalyst spots of Pd−Ir combinations also exhibited bright light at compositions 94:6, 88:12, 81:19, 73:27 at. % (Pd: Ir). Also, the results from optical screening in electrolytes at different $Li^+$ concentrations showed a similar trend as shown in Supporting Information Figures S2 and S3. To verify the reliability of the results from optical screening, multielectrode half-cell test was performed and shown in Supporting Information Figure S4, which had a similar tendency of ORR performance compared to that of optical screening. The composition of 88:12 at. % (Pd: Ir) emitted the highest brightness among the Pd−Ir combinations, which was also supported by the results from multielectrode half-cell test. The selected composition was prepared into single catalyst for further characterization.


dx.doi.org/10.1021/co500041n | ACS Comb. Sci. 2014, 16, 670−677

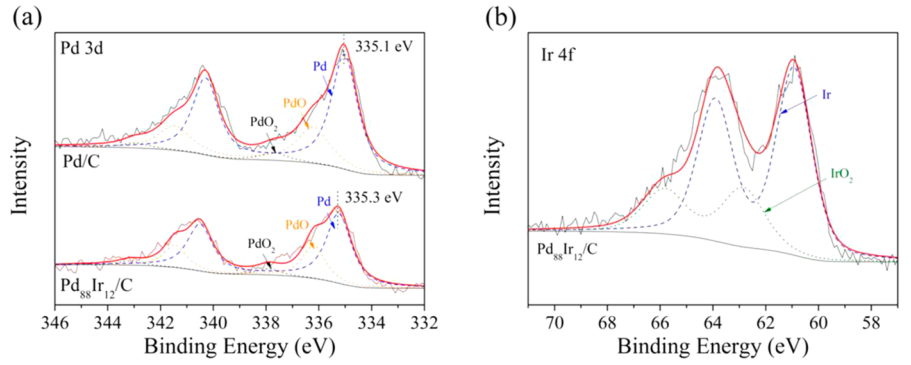


**Figure 3.** (a) XPS-$Pd_{3d}$ and (b) XPS-$Ir_{4f}$ spectroscopy of the prepared catalysts: Pd/C and $Pd_{88}Ir_{12}$/C.

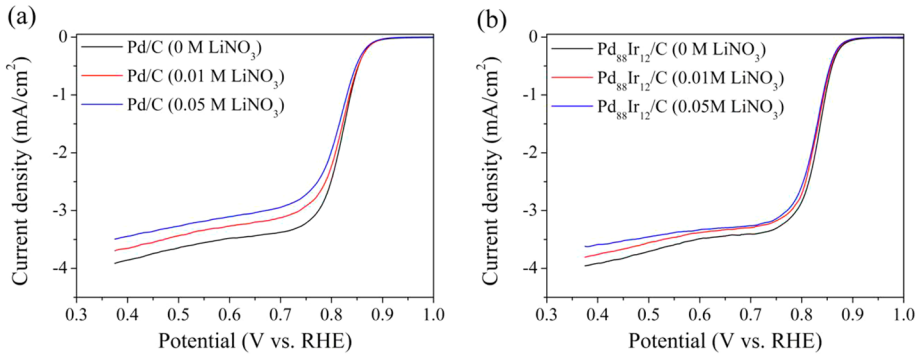


**Figure 4.** Linear sweep voltammetry ORR curves in 0.1 M $HClO_4$ with different $Li^+$ concentrations for (a) Pd/C and (b) $Pd_{88}Ir_{12}$/C.

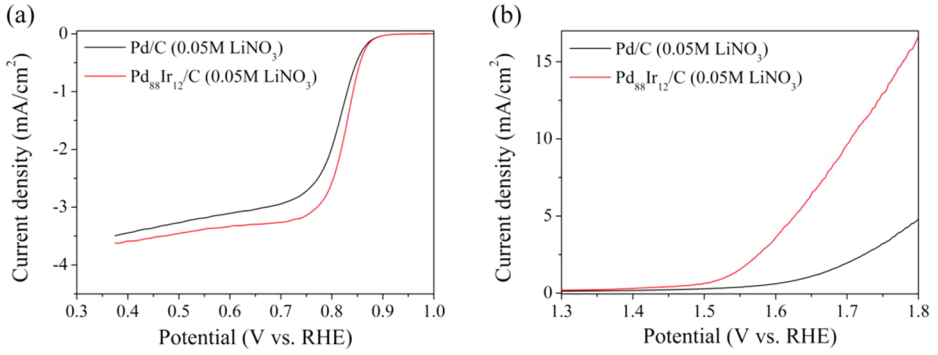


**Figure 5.** Linear sweep voltammetry curves in 0.1 M $HClO_4$ + 0.05 M $LiNO_3$ for Pd/C and $Pd_{88}Ir_{12}$/C (a) ORR performance and (b) OER performance.

The XRD results of the prepared catalysts Pd/C and $Pd_{88}Ir_{12}$/C, are shown in Figure 2. The diffraction peak assigned to the structure (002) was found near 25°.[42] The prepared catalysts show three peaks assigned for the metallic structure (111), (200), and (220). The (111) peak of the $Pd_{88}Ir_{12}$/C catalyst was located at a higher $2\theta$ value (40.4°) compared tothat of the Pd/C catalyst (40.0°). This could correlate with the incorporation of a lower $d$ space crystal structure of Ir ($d_{111}$ = 2.217) than that of Pd ($d_{111}$ = 2.246), suggesting the formation of alloy in the $Pd_{88}Ir_{12}$/C catalyst.[43−45] From the TEM images (Supporting Information Figure S5), the metal particle size between the prepared catalysts Pd/C (2.5 nm) and $Pd_{88}Ir_{12}$/C (2.8 nm) were similar. As the results implied similar metal particle size between the prepared catalysts, this proposed other factors might have altered the electrochemical properties between the prepared catalysts.

XPS analysis of Pd/C and $Pd_{88}Ir_{12}$/C was performed to determine the oxidation states of Pd and Ir at the surface of the catalysts. The XPS results suggested the dominant phase of Pd in the catalysts were metallic Pd when the XPS-$Pd_{3d}$ were deconvoluted by $Pd^0$, PdO and $PdO_2$. The dominant phase of Ir was also analyzed to be metallic Ir by the deconvolution of the $Ir_{4f}$ peak by $Ir^0$ and $IrO_2$. The small amounts of oxides for Pd and Ir found in the XPS data could be due to the exposure of oxygen on the catalyst surface. From Figure 3a, the XPS-$Pd_{3d}$ results showed the binding energies at 335.1 and 335.3 eV for Pd/C and $Pd_{88}Ir_{12}$/C, respectively. The binding energy of Pd in $Pd_{88}Ir_{12}$/C catalyst had an upshift by 0.2 eV compared to that of Pd/C. This upshift in XPS-$Pd_{3d}$ peak suggests the electron modification in the $Pd_{88}Ir_{12}$/C catalyst. This shift in binding energies is in accordance to the electron affinities of Pd (54 kJ/mol) and Ir (112 kJ/mol), which means Pd has electron donating properties compared to Ir.[46,47]


dx.doi.org/10.1021/co500041n | ACS Comb. Sci. 2014, 16, 670−677

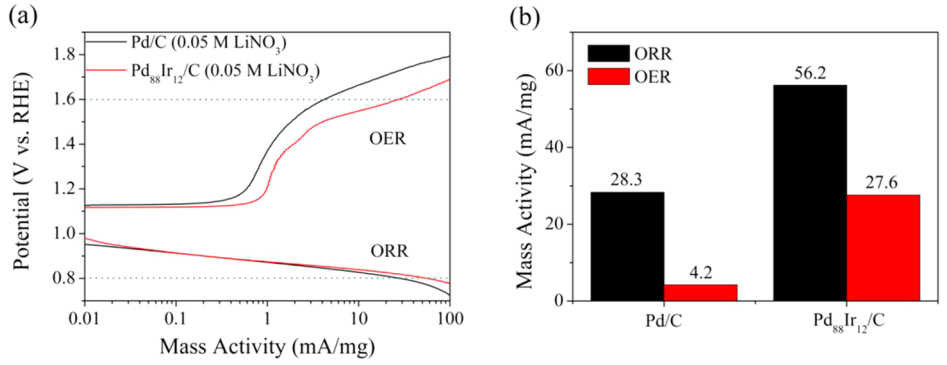


**Figure 6.** (a) Tafel plots, (b) mass activity at 0.8 and 1.6 V (vs RHE) in 0.1 M $HClO_4$ + 0.05 M $LiNO_3$ for Pd/C and $Pd_{88}Ir_{12}$/C.

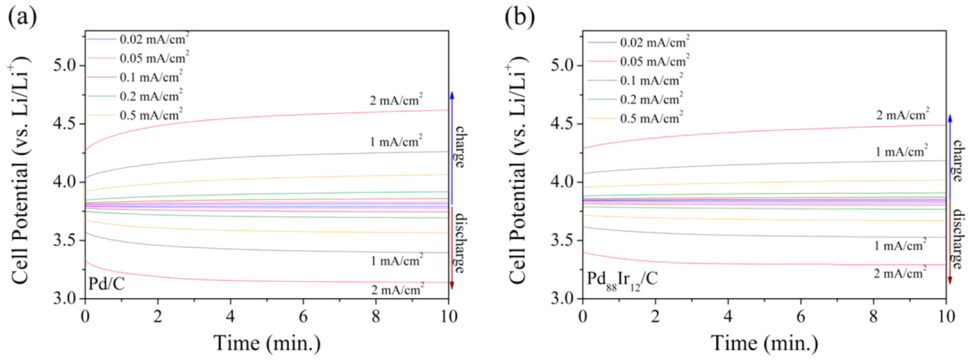


**Figure 7.** Cell voltage profiles at different current densities ranging from 0.02 to 2 mA/$cm^2$ for (a) Pd/C and (b) $Pd_{88}Ir_{12}$/C during discharge and charge.

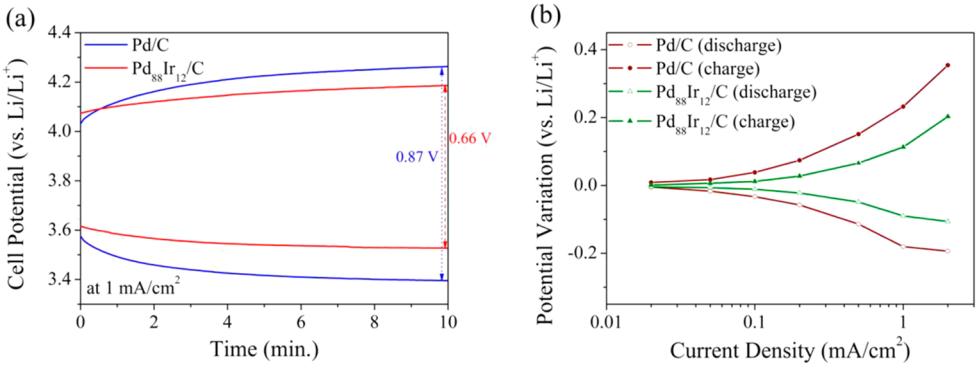


**Figure 8.** (a) Cell voltage profiles at a current density of 1 mA/$cm^2$ for Pd/C, $Pd_{88}Ir_{12}$/C during discharge (lower parts) and charge (upper parts). (b) Polarization curves at different current densities ranging from 0.02 to 2 mA/$cm^2$ for Pd/C and $Pd_{88}Ir_{12}$/C during discharge and charge.

After the contents of the prepared catalysts were verified by physical characterization, the electrochemical test proceeded. The prepared catalysts from the optical screening were examined to investigate the catalytic performance through linear sweep voltammetry (LSV). In the half reaction of the cathode, oxygen reduction evolution reactions follow the reaction pathway without the $Li^+$, $O_2 + 4e^- + 4H^+ \leftrightarrow 2H_2O$. However, $Li^+$ do exist at the side of the cathode in a hybrid Li–air battery. Therefore, $LiNO_3$ (Li salt) was added in the electrolyte to verify the catalytic performance of the prepared catalysts in the presence of $Li^+$. Figure 4 shows the ORR performance of Pd/C and $Pd_{88}Ir_{12}$/C catalysts in 0.1 M $HClO_4$ with different $Li^+$ concentrations as indicated by the figure caption. Both catalysts have a tendency that the diffusion limited current density decreased with increasing $Li^+$ concentrations. This is attributed to the lower rate of oxygen diffusion in the acidic electrolyte containing more $Li^+$.[48] However, each catalyst did not indicate a noticeable variation of onset potential with increasing $Li^+$ concentrations. Also, the oxygen evolution reaction (OER) performance of prepared catalysts in 0.1 M $HClO_4$ with different $Li^+$ concentrations shows a similar tendency with the ORR performance in Supporting Information Figure S6. In Figure 5, the catalytic performance of the prepared catalysts was compared in the presence of $Li^+$, 0.1 M $HClO_4$ + 0.05 M $LiNO_3$. The $Pd_{88}Ir_{12}$/C catalyst has a slightly higher onset potential in ORR than that of Pd/C. At 0.8 V (vs RHE), Pd/C shows a current density of $-1.96$ mA $cm^{-2}$, whereas $Pd_{88}Ir_{12}$/C shows a current density of $-2.58$ mA $cm^{-2}$. In the case of OER, the $Pd_{88}Ir_{12}$/C catalyst shows a higher current density (3.60 mA $cm^{-2}$) at 1.6 V (vs RHE) compared to that of Pd/C (0.61 mA $cm^{-2}$). Furthermore, the ORR and OER performances of the prepared


dx.doi.org/10.1021/co500041n | ACS Comb. Sci. 2014, 16, 670–677

catalysts were estimated by Tafel plot in Figure 6a. Mass activities toward ORR and OER at 0.8 and 1.6 V (vs RHE) were obtained by Tafel plot. As shown in Figure 6b, the $Pd_{88}Ir_{12}/C$ has higher values of mass activity compared to that of Pd/C in both cases.

To investigate the polarization of the hybrid cell with the prepared catalysts, cell voltage was examined under constant current density during discharge and charge. Figure 7 shows the voltage profiles for $Pd_{88}Ir_{12}/C$ and Pd/C, at different current densities ranging from 0.02 to 2 mA $cm^{-2}$. Although the voltage gap between discharge and charge is very small at low current densities for both catalysts, $Pd_{88}Ir_{12}/C$ indicates a smaller voltage gap than that of Pd/C at over 0.2 mA $cm^{-2}$. Also, the voltage profiles of $Pd_{88}Ir_{12}/C$ and Pd/C at a current density of 1 mA $cm^{-2}$ are compared in Figure 8a. After 10 min, $Pd_{88}Ir_{12}/C$ had only 0.66 V gap between the discharge and charge potential compared to that of Pd/C (0.87 V). The cell with $Pd_{88}Ir_{12}/C$ showed a charging potential at around 4.1−4.2 V, which was approximately 0.1 V lower than that of the cell with Pd/C. The cell with $Pd_{88}Ir_{12}/C$ demonstrated a higher discharging potential and this can be deduced from the alloying with Ir,[49] which altered the electron configuration of Pd. The upshift in XPS-$Pd_{3d}$ of $Pd_{88}Ir_{12}/C$ catalyst implies the energy decrease in the d-band center, reducing the oxygen active site adsorption energy. This alternation in the adsorption of oxygen molecules to the $Pd_{88}Ir_{12}/C$ catalyst could have affected the discharge and charge performance.

Wang et al.[50] reported hybrid Li−air battery system using graphene-supported $CoMn_2O_4$ spinel nanoparticles as catalyst in alkaline media. They showed a 0.3 V gap with a current density of 0.025 mA $cm^{-2}$ compared to a 1.0 V gap in carbonate-based Li−air battery (nonaqueous system). However, we found the voltage gap to be less than 0.1 V at the same current density (0.025 mA $cm^{-2}$) in Figure 7. Although, $Pd_{88}Ir_{12}/C$ was applied at a current density of 0.5 mA $cm^{-2}$ which is much higher compared to that of previous reports, the prepared catalyst demonstrated a similar value of voltage gap (0.35 V) between discharge and charge. Moreover, comparing with other previously reported values, the voltage gap of 0.35 V at 0.5 mA $cm^{-2}$ was much lower compared to Yoo et al.[7] (0.56 V at 0.5 mA $cm^{-2}$) and Zhou et al.[51] (0.7 V at 0.5 mA $cm^{-2}$).

Figure 8b shows how much the hybrid Li−air battery is polarized after 10 min. It could be observed that both catalysts have a tendency which the values of voltage variation were increased with increasing applied current density. However, $Pd_{88}Ir_{12}/C$ indicates that the voltage variation is much lower than that of Pd/C, at the measured current densities. This is consistent with the results mentioned above in Figures 7 and 8. Therefore, the hybrid prepared with $Pd_{88}Ir_{12}/C$ had a lower polarization than that with Pd/C.

In conclusion, this study investigates for the first time, the application of combinatorial high-throughput screening method to find the optimized Pd-based catalyst in the hybrid Li−air battery. Though Pd is one-third the cost of Pt, Pd alone struggles to substitute Pt; hence, various combinations and compositions with other metals were investigated toward ORR. From the results obtained by the combinatorial high-throughput screening of the Pd-based binary library, the composition at 88:12 at. % (Pd/Ir) had a trend to emit the brightest light among the catalysts. The ORR and OER performances of the prepared catalyst at the chosen composition were measured and the $Pd_{88}Ir_{12}/C$ catalyst showed a current density of −2.58 mA $cm^{-2}$ at 0.8 V (vs RHE), which was 30% higher than that of Pd/C (−1.97 mA $cm^{-2}$). Furthermore, $Pd_{88}Ir_{12}/C$ catalyst showed a current density of 3.60 mA $cm^{-2}$ at 1.6 V (vs RHE), which was six times higher than that of Pd/C (0.61 mA $cm^{-2}$). A single cell operated for 10 min at 1 mA $cm^{-2}$ with $Pd_{88}Ir_{12}/C$ at the cathode, had a smaller voltage gap (0.66 V) between the charge and the discharge which had a 30% higher energy efficiency compared to that of a cell prepared with Pd/C (0.87 V). In this experiment, the results from combinatorial high-throughput screening method facilitated the search for highly active catalyst; therefore, this method could be further applied in the field of Li−air battery.

## EXPERIMENTAL PROCEDURES

The carbon spots in the combinatorial library were prepared by spraying a prepared carbon ink on a polytetrafluoroethlyene (PTFE) treated carbon paper (Toray TGPH-090, 20 wt % PTFE). Each spot had a diameter of 4 mm and 6 mm apart from each other as the design scheme as shown in Figure 9.

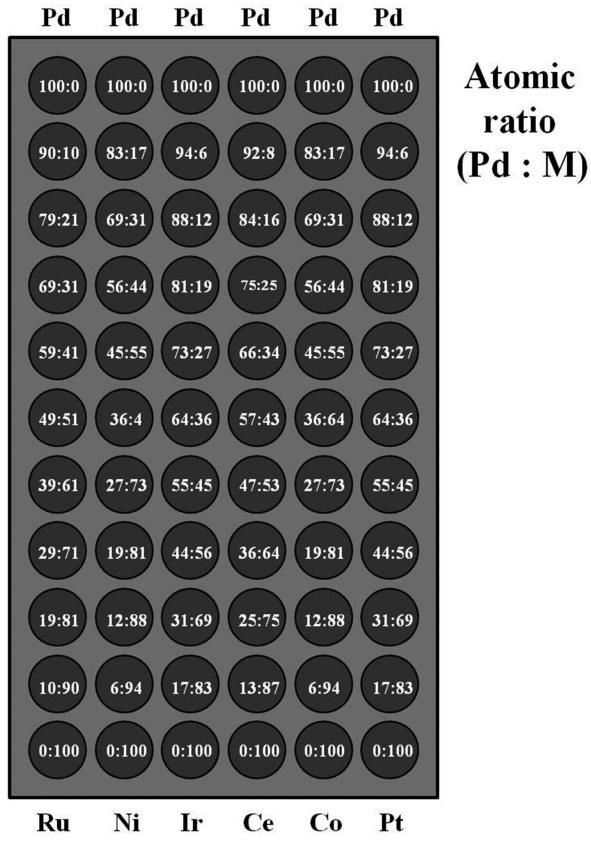


**Figure 9.** Design of Pd-based combinatorial library.

The carbon ink was prepared by a mixture of Ketjen black (0.1 g), deionized (DI) water (120 μL), 5 wt % Nafion ionomer solution (970 μL), and isopropyl alcohol (5 mL). The loading of carbon alone in each spot was estimated to 0.15 mg. Calculated amounts of catalyst precursor solutions were dropped at each spot with loading adjustment of metal on carbon to 40 wt %. Ruthenium chloride ($RuCl_3$), palladium chloride ($PdCl_2$), nickel nitrate ($Ni(NO_3)_2{\cdot}6H_2O$), iridium chloride ($IrCl_3$), cerium nitrate ($Ce(NO_3)_3{\cdot}6H_2O$), cobalt chloride ($CoCl_2{\cdot}6H_2O$), and chloroplatinic acid ($H_2PtCl_6$) were used as metal precursors for the selected metals. After calculated amounts of metal precursor solutions were loaded,


dx.doi.org/10.1021/co500041n | ACS Comb. Sci. 2014, 16, 670−677

the combinatorial library was dried at room temperature overnight. Then the precursors in the catalyst spots were reduced by immersing the library in 0.2 M $NaBH_4$ solution for 2 h. After reduction, the library was washed and dried.

The prepared combinatorial library was used as a working electrode in the analysis of optical screening.[29] Optical screening requires an electrolyte with the properties of a UV sensitive pH indicator. From previous reports, fluorescein Na salt was used as the pH indicator to investigate the ORR performance of the catalyst spots in combinatorial library.[34,36] Other indicators other than fluorescein Na salt, were also examined for its practicability in optical screening in the presence of Li salt (Supporting Information Table S1.). Out of the possible indicator candidates fluorescein Na salt was selected as the most viable. $NaNO_3$ was selected to reduce the conduction resistance in the electrolyte. The prepared electrolyte consisted of 100 $\mu$M fluorescein Na salt and 0.2 M $NaNO_3$ with a pH adjusted to 4 and purged with oxygen. Additionally, $LiNO_3$ as a Li salt added in the electrolyte to verify the ORR performance of the prepared catalysts in the presence of $Li^+$. Optical screening was carried out inside a homemade glovebox with a UV light source and a camera as shown in Figure 10. A

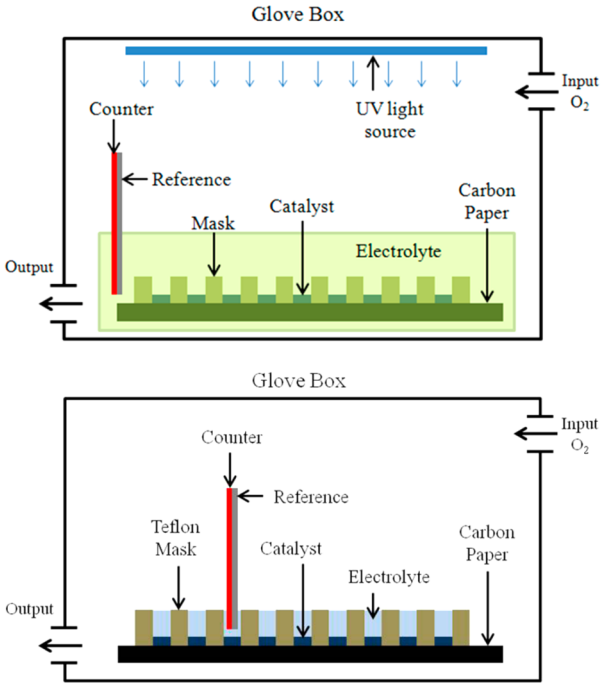


**Figure 10.** Scheme of optical screening method (upper) and multielectrode half-cell method (lower).

constant potential of 0.8 V (vs RHE) was applied to the combinatorial library (the working electrode) under UV light. In previous report, the catalyst spots with higher ORR performance consume $H^+$ faster than other catalyst spots with low ORR performance, consequently, the pH of the electrolyte will increase because of the consumption of $H^+$.[28] The used electrolyte is excited under UV light when the pH is higher than 4.5.[31] Therefore, electrolyte near the catalyst spots that have higher ORR performance would emit light faster.

In the electrochemical tests, including the combinatorial library and the single catalysts, a platinum wire (ALS Co., 002233) and an Ag/AgCl electrode (ALS CO., 012167) were used as the counter and the reference electrodes, respectively. All electrochemical tests were carried out using an electrochemical analyzer (CH Instruments, Inc. CHI700D). The multielectrode half-cell method is similar to the three electrode half-cell test, consisting of a working, a counter and a reference electrode as shown in Figure 10. In this methodology, the prepared combinatorial library was used as working electrode. To measure the ORR performance of each catalyst spots, a PTFE mask with 66 holes (each hole on each catalyst spot on the combinatorial library) of 5 mm diameter and 10 mm depth is used for electrolyte isolation. The counter and reference electrodes were put into each hole. This process was repeated for each and every spot on the library. The ORR performance of catalyst spots was analyzed by linear sweep voltammetry between 1.04 to 0.7 V (vs RHE) at an oxygen purged 0.1 M $HClO_4$ electrolyte with different concentrations of Li salt (0, 0.01, 0.05 M $LiNO_3$).

Single catalysts were prepared with respect to the results from optical screening. To maintain similarities within the preparation of the catalysts, single catalysts were also prepared by the impregnation with $NaBH_4$.[34,35] Ketjen black (0.1 g) was dispersed in a mix solution of 200 mL of DI-water and 100 mL of isopropyl alcohol (IPA). Calculated amounts of the chosen metal precursor solutions were added to the solution and stirred for 30 min. The $NaBH_4$ was 10-fold mole of the total metal precursor added in 100 mL of DI-water and mixed to catalyst solution. The mixed solution was stirred for 2 h and filtered. The product was washed several times with DI-water and dried overnight in a vacuum oven at 70 °C. Pd/C was also prepared using the same method for comparison.

The electrochemical properties of the prepared catalysts were analyzed using a three-electrode beaker cell equipped with a Pt wire counter-electrode (ALS Co., 002233), an Ag/AgCl reference electrode (ALS Co., 012167), and a rotating ring disk electrode (ALS Co., 011162). Electrochemical analyzer (CHI700D, CH Instruments Inc.) and a rotator (RRDE-3A, ALS Co.) were used. The working electrodes were prepared using the thin film electrode method. The catalysts (10 mg) were dispersed in ink solution of 1 mL (DI-water (15), 5 wt % Nafion in water (4), and isopropyl alcohol (1); the number in parentheses indicates the volumetric ratio) followed by sonication, respectively. Then, each catalyst inks (5 $\mu$L) were dropped onto the glassy carbon of a rotating ring disk electrode (RRDE). The catalyst inks were dried at room temperature. 100 cycles of the cyclic voltammetry (CV) was conducted in deaerated 0.1 M $HClO_4$ electrolyte in order to activate the catalysts with a 40 $mVs^{-1}$ scan rate from 0.074 to 1.294 V (vs RHE). The data from the last cycle was selected for comparison. The ORR experiments were proceeded in an $O_2$ saturated variable concentration of Li salt in 0.1 M $HClO_4$ electrolyte with a 5 $mVs^{-1}$ scan rate and 900 rpm rotating velocity from 1.114 to 0.374 V (vs RHE). Additionally, the OER experiments were proceeded from 1.1 to 1.849 V (vs RHE).

The prepared catalysts were applied to hybrid Li–air cell which consists of Li metal|$LiPF_6$ in 1:1 of ethylene carbonate (EC)/dimethyl carbonate (DMC)|LTAP solid electrolyte|1 M $LiNO_3$ in 0.01 M $HClO_4$|cathode. Cathode consisted of the prepared catalysts, Ketjen black, PTFE (weight ratio of 40:50:10, respectively). The nonaqueous electrolyte (EC:DMC) was used with a glass-fiber separator at the side of the anode, the aqueous electrolyte (0.01 M $HClO_4$ with 1 M $LiNO_3$) was used at the side of the cathode. These electrolytes were separated by a Li-ion solid electrolyte (LTAP) from


dx.doi.org/10.1021/co500041n | ACS Comb. Sci. 2014, 16, 670–677

OHARA, Inc., Japan. The hybrid Li−air cell was tested at various current densities, ranging from 0.02 to 2 mA $cm^{-2}$.

Physical characterizations of the single catalysts were performed by X-ray diffraction (XRD) and X-ray photoelectron spectroscopy (XPS). XRD patterns were acquired using a D/MAX-2500 (RIgaku) operating a 40 kV and 300 mA, with step-scan patterns between 10 to 70° (2$\theta$ range) with 0.01° step size and 1° $min^{-1}$ scan speed. XPS analysis were tested using a Sigma Probe (Thermo VG Scientific) equipped with a microfocused monochromator X-ray source.

## ■ ASSOCIATED CONTENT

### Supporting Information

Full images from optical screening (with or without Li salt), the ORR results of the multielectrode half cell test, TEM images of prepared catalysts, and the OER results of prepared catalysts (with or without Li salt). This material is available free of charge via the Internet at http://pubs.acs.org.

## ■ AUTHOR INFORMATION


### Corresponding Author

*E-mail: siwoo@kaist.ac.kr.

### Author Contributions

§Y.J.J. and S.H.P. are both first authors and contributed equally.


### Notes

The authors declare no competing financial interest.

## ■ ACKNOWLEDGMENTS

This work was supported by the Energy Efficiency & Resources of the Korea Institute of Energy Technology Evaluation and Planning (No. 20112020100110) grant funded by the Korea government Ministry of Knowledge Economy

## ■ REFERENCES


(1) Girishkumar, G.; M, B.; Luntz, A. C.; Swanson, S.; Wilcke, W. Lithium−Air Battery: Promise and Challenges. *J. Phys. Chem. Lett.* **2010**, *1*, 2193−2203.

(2) Cheng, F. Y.; Chen, J. Metal−Air Batteries: From Oxygen Reduction Electrochemistry to Cathode Catalysts. *Chem. Soc. Rev.* **2012**, *41* (6), 2172−2192.

(3) Yang, X. H.; He, P.; Xia, Y. Y. Preparation of Mesocellular Carbon Foam and Its Application for Lithium/Oxygen Battery. *Electrochem. Commun.* **2009**, *11* (6), 1127−1130.

(4) Freunberger, S. A.; Chen, Y. H.; Peng, Z. Q.; Griffin, J. M.; Hardwick, L. J.; Barde, F.; Novak, P.; Bruce, P. G. Reactions in the Rechargeable Lithium-O-2 Battery with Alkyl Carbonate Electrolytes. *J. Am. Chem. Soc.* **2011**, *133* (20), 8040−8047.

(5) Armand, M.; Tarascon, J. M. Building Better Batteries. *Nature* **2008**, *451* (7179), 652−657.

(6) Wang, Y. G.; Zhou, H. S. A Lithium−Air Fuel Cell Using Copper to Catalyze Oxygen-Reduction Based on Copper-Corrosion Mechanism. *Chem. Commun.* **2010**, *46* (34), 6305−6307.

(7) Yoo, E.; Zhou, H. Li−Air Rechargeable Battery Based on Metal-free Graphene Nanosheet Catalysts. *ACS Nano* **2011**, *5*, 3020−3026.

(8) Débart, A.; Paterson, A. J.; Bao, J.; Bruce, P. G. $\alpha$-$MnO_2$ Nanowires: A Catalyst for the $O_2$ Electrode in Rechargeable Lithium Batteries. *Angew. Chem., Int. Ed.* **2008**, *47* (24), 4521−4524.

(9) Lu, Y.-C.; Xu, Z.; Gasteiger, H. A.; Chen, S.; Hamad-Schifferli, K.; Yang, S.-H. Platinum-Gold Nanoparticles: A Highly Active Bifunctional Electrocatalyst for Rechargeable Lithium-Air Batteries. *J. Am. Chem. Soc.* **2010**, *132*, 12170−12171.

(10) Débart, A.; Bao, J.; Armstrong, G.; Bruce, P. G. An $O_2$ Cathode for Rechargeable Lithium Batteries: The Effect of a Catalyst. *J. Power Sources* **2007**, *174* (2), 1177−1182.

(11) Guo, J. S.; Hsu, A.; Chu, D.; Chen, R. R. Improving Oxygen Reduction Reaction Activities on Carbon-Supported Ag Nanoparticles in Alkaline Solutions. *J. Phys. Chem. C* **2010**, *114* (10), 4324−4330.

(12) Peng, Z.; Freunberger, S. A.; Chen, Y.; Bruce, P. G. A Reversible and Higher-Rate Li-$O_2$ Battery. *Science* **2012**, *337*, 563−566.

(13) Lim, B.; Jiang, M. J.; Camargo, P. H. C.; Cho, E. C.; Tao, J.; Lu, X. M.; Zhu, Y. M.; Xia, Y. N. Pd−Pt Bimetallic Nanodendrites with High Activity for Oxygen Reduction. *Science* **2009**, *324* (5932), 1302−1305.

(14) Li, Y.; Wang, J.; Li, X.; Geng, D.; Li, R.; Sun, X. Superior Energy Capacity of Graphene Nanosheets for a Nonaqueous Lithium−Oxygen Battery. *Chem. Commun.* **2011**, *47*, 9438−9440.

(15) Mitchell, R. R.; Gallant, B. M.; Thompson, C. V.; Shao-Horn, Y. All-Carbon-Nanofiber Electrodes for High-Energy Rechargeable Li−$O_2$ Batteries. *Energy Environ. Sci.* **2011**, *4* (8), 2952−2958.

(16) Yuasa, M.; Nishida, M.; Kida, T.; Yamazoe, N.; Shimanoe, K. Bi-functional Oxygen Electrodes Using $LaMnO_3$/$LaNiO_3$ for Rechargeable Metal−Air Batteries. *J. Electrochem. Soc.* **2011**, *158* (5), A605−A610.

(17) Cheng, F.; Shen, J.; Peng, B.; Pan, Y.; Tao, Z.; Chen, J. Rapid room-temperature synthesis of nanocrystalline spinels as oxygen reduction and evolution electrocatalysts. *Nat. Chem.* **2011**, *3*, 79−84.

(18) Suntivich, J.; Gasteiger, H. A.; Yabuuchi, N.; Nakanishi, H.; Goodenough, J. B.; Shao-Horn, Y. Design Principles for Oxygen-Reduction Activity on Perovskite Oxide Catalysts for Fuel Cells and Metal−Air Batteries. *Nat. Chem.* **2011**, *3*, 546−550.

(19) Bashyam, R.; Zelenay, P. A Class of Non-precious Metal Composite Catalysts for Fuel Cells. *Nature* **2006**, *443* (7107), 63−66.

(20) Lefèvre, M.; Proietti, E.; Jaouen, F.; Dodelet, J.-P. Iron-Based Catalysts with Improved Oxygen Reduction Activity in Polymer Electrolyte Fuel Cells. *Science* **2009**, *324* (5923), 71−74.

(21) Wu, G.; More, K. L.; Johnston, C. M.; Zelenay, P. High-Performance Electrocatalysts for Oxygen Reduction Derived from Polyaniline, Iron, and Cobalt. *Science* **2011**, *332* (6028), 443−447.

(22) Lee, K. R.; Jung, Y.; Woo, S. I. Combinatorial Screening of Highly Active Pd Binary Catalysts for Electrochemical Oxygen Reduction. *Acs Comb. Sci.* **2012**, *14* (1), 10−16.

(23) Zhang, L.; Lee, K.; Zhang, J. The Effect of Heat Treatment on Nanoparticle Size and ORR Activity for Carbon-Supported Pd−Co Alloy Electrocatalysts. *Electrochim. Acta* **2007**, *52* (9), 3088−3094.

(24) Li, X.; Huang, Q.; Zou, Z.; Xia, B.; Yang, H. Low Temperature Preparation of Carbon-Supported PdCo Alloy Electrocatalysts for Methanol-Tolerant Oxygen Reduction Reaction. *Electrochim. Acta* **2008**, *53* (22), 6662−6667.

(25) Ramos-Sánchez, G.; Yee-Madeira, H.; Solorza-Feria, O. PdNi Electrocatalyst for Oxygen Reduction in Acid Media. *Int. J. Hydrogen Energy* **2008**, *33* (13), 3596−3600.

(26) Shao, M.-H.; Sasaki, K.; Adzic, R. R. Pd−Fe Nanoparticles as Electrocatalysts for Oxygen Reduction. *J. Am. Chem. Soc.* **2006**, *128* (11), 3526−3527.

(27) Sarkar, A.; Murugan, A. V.; Manthiram, A. Synthesis and Characterization of Nanostructured Pd−Mo Electrocatalysts for Oxygen Reduction Reaction in Fuel Cells. *J. Phys. Chem. C* **2008**, *112* (31), 12037−12043.

(28) Reddington, E.; Sapienza, A.; Gurau, B.; Viswanathan, R.; Sarangapani, S.; Smotkin, E. S.; Mallouk, T. E. Combinatorial Electrochemistry: A Highly Parallel, Optical Screening Method for Discovery of Better Electrocatalysts. *Science* **1998**, *280* (5370), 1735−1737.

(29) Jeon, M. K.; Liu, J. H.; Lee, K. R.; Lee, J. W.; McGinn, P. J.; Woo, S. I. Combinatorial Search for Quaternary Methanol Tolerant Oxygen Electro-Reduction Catalyst. *Fuel Cells* **2010**, *10* (1), 93−98.

(30) Lee, K. R.; Jeon, M. K.; Woo, S. I. Composition Optimization of PtRuM/C (M = Fe and Mo) Catalysts for Methanol Electro-oxidation via Combinatorial Method. *Appl. Catal., B* **2009**, *91* (1−2), 428−433.

(31) Liu, J. H.; Jeon, M. K.; Woo, S. I. High-Throughput Screening of Binary Catalysts for Oxygen Electroreduction. *Appl. Surf. Sci.* **2006**, *252* (7), 2580−2587.

(32) Chan, B. C.; Liu, R. X.; Jambunathan, K.; Zhang, H.; Chen, G. Y.; Mallouk, T. E.; Smotkin, E. S. Comparison of High-Throughput Electrochemical Methods for Testing Direct Methanol Fuel Cell Anode Electrocatalysts. *J. Electrochem. Soc.* **2005**, *152* (3), A594−A600.
(33) Chen, G.; Delafuente, D. A.; Sarangapani, S.; Mallouk, T. E. Combinatorial Discovery of Bifunctional Oxygen Reduction—Water Oxidation Electrocatalysts for Regenerative Fuel Cells. *Catal. Today* **2001**, *67* (4), 341−355.
(34) Cooper, J. S.; McGinn, P. J. Combinatorial Screening of Thin Film Electrocatalysts for a Direct Methanol Fuel Cell Anode. *J. Power Sources* **2006**, *163* (1), 330−338.
(35) Gurau, B.; Viswanathan, R.; Liu, R.; Lafrenz, T. J.; Ley, K. L.; Smotkin, E. S.; Reddington, E.; Sapienza, A.; Chan, B. C.; Mallouk, T. E.; Sarangapani, S. Structural and Electrochemical Characterization of Binary, Ternary, and Quaternary Platinum Alloy Catalysts for Methanol Electro-oxidation 1. *J. Phys. Chem. B* **1998**, *102* (49), 9997−10003.
(36) Morris, N. D.; Mallouk, T. E. A High-Throughput Optical Screening Method for the Optimization of Colloidal Water Oxidation Catalysts. *J. Am. Chem. Soc.* **2002**, *124* (37), 11114−11121.
(37) Prochaska, M.; Jin, J.; Rochefort, D.; Zhuang, L.; DiSalvo, F. J.; Abruna, H. D.; van Dover, R. B. High Throughput Screening of Electrocatalysts for Fuel Cell Applications. *Rev. Sci. Instrum.* **2006**, *77* (5), No. 054104.
(38) Smotkin, E. S.; Díaz-Morales, R. R. New Electrocatalysts by Combinatorial Methods. *Annu. Rev. Mater. Res.* **2003**, *33* (1), 557−579.
(39) Smotkin, E. S.; Jiang, J.; Nayar, A.; Liu, R. High-Throughput Screening of Fuel Cell Electrocatalysts. *Appl. Surf. Sci.* **2006**, *252* (7), 2573−2579.
(40) Sun, Y.; Buck, H.; Mallouk, T. E. Combinatorial Discovery of Alloy Electrocatalysts for Amperometric Glucose Sensors. *Anal. Chem.* **2001**, *73* (7), 1599−1604.
(41) Park, S. H.; Choi, C. H.; Koh, J. K.; Pak, C.; Jin, S.-a.; Woo, S. I. Combinatorial High-Throughput Screening for Highly Active Pd−Ir−Ce-Based Ternary Catalysts in Electrochemical Oxygen Reduction Reaction. *ACS Comb. Sci.* **2013**, *15* (11), 572−579.
(42) Yang, S. D.; Zhang, X. G.; Mi, H. Y.; Ye, X. G. Pd Nanoparticles Supported on Functionalized Multi-Walled Carbon Nanotubes (MWCNTs) and Electrooxidation for Formic Acid. *J. Power Sources* **2008**, *175* (1), 26−32.
(43) Nguyen, S. T.; Law, H. M.; Nguyen, H. T.; Kristian, N.; Wang, S. Y.; Chan, S. H.; Wang, X. Enhancement Effect of Ag for Pd/C Towards the Ethanol Electro-oxidation in Alkaline Media. *Appl. Catal., B* **2009**, *91* (1−2), 507−515.
(44) Shen, S. Y.; Zhao, T. S.; Xu, J. B. Carbon-Supported Bimetallic PdIr Catalysts for Ethanol Oxidation in Alkaline Media. *Electrochim. Acta* **2010**, *55* (28), 9179−9184.
(45) Wang, Y. G.; Zhou, H. S. A Lithium−Air Battery with a Potential to Continuously Reduce O-2 from Air for Delivering Energy. *J. Power Sources* **2010**, *195* (1), 358−361.
(46) Ziaei-azad, H.; Yin, C.-X.; Shen, J.; Hu, Y.; Karpuzov, D.; Semagina, N. Size- and Structure-Controlled Mono- and Bimetallic Ir−Pd Nanoparticles in Selective Ring Opening of Indan. *J. Catal.* **2013**, *300* (0), 113−124.
(47) Lee, K. H.; Han, S.-W.; Kwon, K.-Y.; Park, J. B. Systematic Analysis of Palladium−Graphene Nanocomposites and Their Catalytic Applications in Sonogashira Reaction. *J. Colloid Interface Sci.* **2013**, *403* (0), 127−133.
(48) Liu, H.; Xing, Y. C. Influence of Li Ions on the Oxygen Reduction Reaction of Platinum Electrocatalyst. *Electrochem. Commun.* **2011**, *13* (6), 646−649.
(49) You, D. J.; Jin, S. A.; Lee, K. H.; Pak, C.; Choi, K. H.; Chang, H. Improvement of Activity for Oxygen Reduction Reaction by Decoration of Ir on PdCu/C Catalyst. *Catal. Today* **2012**, *185* (1), 138−142.
(50) Wang, L.; Zhao, X.; Lu, Y. H.; Xu, M. W.; Zhang, D. W.; Ruoff, R. S.; Stevenson, K. J.; Goodenough, J. B. $CoMn_2O_4$ Spinel Nanoparticles Grown on Graphene as Bifunctional Catalyst for Lithium−Air Batteries. *J. Electrochem. Soc.* **2011**, *158* (12), A1379−A1382.
(51) Zhou, H. S.; Wang, Y. G.; Li, H. Q.; He, P. The Development of a New Type of Rechargeable Batteries Based on Hybrid Electrolytes. *ChemSusChem* **2010**, *3* (9), 1009−1019.